



HAL
open science

Solubilities of Carbon Dioxide and Oxygen in the Ionic Liquids Methyl Trioctyl Ammonium Bis (trifluoromethylsulfonyl) imide, 1-Butyl-3-Methyl Imidazolium Bis (trifluoromethylsulfonyl) imide, and 1-Butyl-3-Methyl Imidazolium Methyl Sulphate

Indra Bahadur, Khalid Osman, Christophe Coquelet, Paramespri Naidoo,
Deresh Ramjugernath

► **To cite this version:**

Indra Bahadur, Khalid Osman, Christophe Coquelet, Paramespri Naidoo, Deresh Ramjugernath. Solubilities of Carbon Dioxide and Oxygen in the Ionic Liquids Methyl Trioctyl Ammonium Bis (trifluoromethylsulfonyl) imide, 1-Butyl-3-Methyl Imidazolium Bis (trifluoromethylsulfonyl) imide, and 1-Butyl-3-Methyl Imidazolium Methyl Sulphate. *Journal of Physical Chemistry B*, 2015, 119 (4), pp.1503-1514. 10.1021/jp5061057. hal-01251051

HAL Id: hal-01251051

<https://minesparis-psl.hal.science/hal-01251051>

Submitted on 5 Jan 2016

HAL is a multi-disciplinary open access archive for the deposit and dissemination of scientific research documents, whether they are published or not. The documents may come from teaching and research institutions in France or abroad, or from public or private research centers.

L'archive ouverte pluridisciplinaire **HAL**, est destinée au dépôt et à la diffusion de documents scientifiques de niveau recherche, publiés ou non, émanant des établissements d'enseignement et de recherche français ou étrangers, des laboratoires publics ou privés.

**Solubilities of Carbon Dioxide and Oxygen in the Ionic Liquids Methyl
Trioctyl Ammonium Bis (trifluoromethylsulfonyl) imide, 1-Butyl-3-Methyl
Imidazolium Bis (trifluoromethylsulfonyl) imide, and 1-Butyl-3-Methyl
Imidazolium Methyl Sulphate**

Indra Bahadur,[†] Khalid Osman,[†] Christophe Coquelet,^{‡, †} Paramespri Naidoo,[†] Deresh
Ramjugernath,^{*, †}

[†]Thermodynamics Research Unit, School of Engineering, University of KwaZulu-Natal,
Howard College Campus, King George V Avenue, Durban, 4041, South Africa

[‡]Mines-Paristech CEP/TEP, 35, rue Saint Honoré, 77305 Fontainebleau, France

***Corresponding author – E-mail: ramjuger@ukzn.ac.za**

ABSTRACT:

Ionic liquids (ILs) are being considered as solvents for gas absorption processes as they have the potential, in general, for improved efficiency of gas separations, as well as lower capital and operating costs compared to current commercial processes. In this study the solvent properties of ILs are investigated for use in the absorption of carbon dioxide (CO₂) and oxygen (O₂). The absorption of these gases in ILs was measured in a temperature range of 303.15 to 333.15 K and at pressures up to 1.5 MPa by gravimetric analysis. The ILs used were: methyl trioctyl ammonium bis (trifluoromethylsulfonyl) amide [MOA][Tf₂N], 1-butyl-3-methyl imidazolium bis (trifluoromethylsulfonyl) amide [BMIM][Tf₂N] and 1-butyl-3-methyl imidazolium methyl sulphate [BMIM][MeSO₄]. The measurement technique employed in this study is fast, accurate, and requires small quantities of solvent. The results indicated that absorption of both gases increased with a decrease in operating temperature and an increase in pressure. [MOA][Tf₂N] had the highest CO₂ and O₂ solubility. [BMIM][Tf₂N] was determined to have the highest selectivity for CO₂ absorption. [BMIM][MeSO₄] achieved the lowest CO₂ absorption with a moderate O₂ absorption, revealing this IL to be the least desirable for CO₂ and O₂ absorption. Calculation of Henry's law constants for both gases in all ILs at all isotherms confirmed the deductions made from absorption data analysis. The absorption data was modelled using the generic Redlich-Kwong cubic equation of state (RK-EOS) coupled with a group contribution method.

Keywords: carbon dioxide; oxygen; gas solubility; gravimetric analysis; ionic liquids

1. INTRODUCTION

Recent research has shown that the main contributor to an increased rate and extent of global climate change, are CO₂ emissions from various fossil fuel industries including fossil fuel-fired power plants, coal-to-liquids (CTL) and gas-to-liquids (GTL) industries, steel and cement industries.³ Thus, numerous studies have been undertaken to investigate different techniques for capturing CO₂ from flue gas emitted by these industries, and thereafter storing the CO₂ underground or by other means, thereby preventing its emission into the atmosphere. Despite significant research however, a technique with low energy penalty to feasibly capture CO₂ still remains to be found.

A common CO₂ capture technique closest to commercialisation is the use of solvents to selectively absorb CO₂ from flue gas emitted by fossil fuel industries. Current and conventional solvents include alkanolamines and carbonate-based solvents. These solvents however possess numerous disadvantages, including high corrosiveness, low absorption capacity and high energy requirements for desorption and recycling. Moreover, these solvents have proven to be volatile under industrial flue gas conditions, which has serious repercussions with regard to human health and the environment.^{1,2} In some cases, the adverse effects of these solvents on human health, safety, and the environment, combined with their volatility and flammability, has led to legislation to minimize their use.⁴

A relatively new type of solvent known as ionic liquids, has received much attention in recent years. Ionic liquids are molten salts that typically have melting points below 373.15 K.⁸ The specific advantages of ionic liquids is that many can be tuned to have negligible vapour pressure,⁹ good dissolution characteristics,¹⁰ and are non-flammable¹¹ and non-toxic¹², depending on the cation and anion used. It is for these reasons, that many ionic liquids have

been regarded as “green” solvents, which can possibly replace more hazardous conventional solvents in many chemical processes, including CO₂ capture⁵⁻⁷. There are literally thousands of ionic liquids which can be synthesized, tested, and optimized for thermal, mechanical and chemical stability, and suitable density for various applications.¹⁴

Gas absorption measurements in ionic liquids can provide information about the interaction such as dipole-dipole interactions that exist between these gases and ionic liquids.²² These studies can also provide important information about the original solvent behaviour of ionic liquids.²² Absorption data for many gas-ionic liquid systems are scarce compared to systems utilising conventional physical and chemical solvents. Research has however been conducted at an accelerated pace as the potential of ionic liquids becomes known.²³⁻³²

Numerous sources in literature have investigated ionic liquids for their absorption capacity of CO₂. CO₂ mole fractions were measured by gravimetric analysis in a variety of fluorinated and non-fluorinated ionic liquids at temperatures of 283.15-333.15 K and pressures up to 90 bar by Anderson et al.⁵⁰ and Muldoon et al.³⁴. Significant focus was made on CO₂ mole fraction measurement in non-fluorinated ionic liquids by Palgunadi et al.³⁵ and Zhang et al.³⁷, at atmospheric pressure and temperatures of 298.15-334.15 K. Shiflett and Yokozeki⁴⁹, Arshad³⁸, and Hasib-ur-Rahman et al.³⁹ considered fluorinated imidazolium-based ionic liquids in their studies, at temperatures of 298.15-348.15 K and 0.1-800 bar. Anderson et al.⁵⁰ utilised a Rubotherm for high pressure VLE measurement.

The aim of this study was to measure CO₂ and O₂ absorption in Methyl trioctyl ammonium bis (trifluoromethylsulfonyl) imide ([MOA][Tf₂N]), 1-butyl-3-methyl imidazolium bis (trifluoromethylsulfonyl) imide ([BMIM][Tf₂N]) and 1-butyl-3-methyl imidazolium methyl sulphate ([BMIM][MeSO₄]). While CO₂ absorption in [BMIM][Tf₂N] is well measured³⁴, O₂ absorption has not. The measurement of O₂ absorption is important since flue gas from coal power plants may contain up to 5% unreacted O₂ (by volume), and solvents need to be highly CO₂ selective to enable the efficient recovering of pure CO₂ for disposal. Moreover, CO₂ and O₂ absorption in the relatively new ionic liquids had not been measured previously.

Absorption measurements were performed by gravimetric analysis using an Intelligent Gravimetric Analyser (IGA-001) to determine the absorption isotherm of CO₂ and O₂ in the above three ionic liquids .at temperatures of 303.15, 313.15, 323.15 and 333.15 K and pressures up to 1.5 MPa. The Henry's law constant for both gases in all ionic liquids at all isotherms were calculated. The absorption data was modelled using a generic RK-EOS with the aid of a group contribution method. The 3D structure of the ionic liquids is given in Figure 1. The effect of cation, anion and the operating conditions on absorption of CO₂ and O₂ in fluorinated and non-fluorinated ionic liquids were analysed, together with the CO₂ selectivity of each ionic liquid over O₂.

2. EXPERIMENTAL PROCEDURE

2.1 Materials

Carbon dioxide (CO₂) and oxygen (O₂) were obtained from Afrox Ltd (South Africa) with a minimum purity of 99.9 %. The ionic liquids: [MOA][Tf₂N] was obtained from Fluka,

[BMIM][Tf₂N] and [BMIM][MeSO₄] were obtained from Sigma-Aldrich, with a minimum purity of 98.0 %. Characterization of the chemicals is provided in Table 1.

2.2 Experimental Procedure

2.2.1 Density and Refractive Index Measurements

The measurements of density (ρ) and refractive index (n) of the pure ionic liquids were undertaken using a digital vibrating-tube densimeter (Anton Paar DMA 5000) and refractometer (ATAGO, model RX-7000a, Japan), respectively with an accuracy of ± 0.03 K in temperature. The estimated accuracy in density and refractive index was ± 0.00003 g·cm⁻³ and ± 0.00005 , respectively. The experimental density (ρ) and refractive index (n) of pure ionic liquids together with literature^{8,33,36} densities (ρ) and refractive index (n) are given in Table 1. Moreover, the water content was determined using a Metrohm 702 SM Titrino Meter and was found to be 400 ppm in [MOA][Tf₂N], 600 ppm in [BMIM][Tf₂N] and 500ppm in [BMIM][MeSO₄]. Samples were degassed before measurement as explained below.

2.2.2 Gas Absorption and Desorption Measurements

Gas absorption and desorption measurements of various gases in ionic liquids were conducted by gravimetric analysis using an Intelligent Gravimetric Analyser (IGA-001) built by Hiden Analytical Ltd. A quantity of approximately 70 to 100 mg of solvent was typically loaded onto a stainless steel sample holder which was then loaded into a stainless steel reactor. The sample holder was attached to tungsten and gold wire leading up to a microbalance which has a resolution of ± 0.001 mg. The weight of the sample holder is countered using a counterweight so that only the sample weight may be tracked.

Each sample was degassed in the apparatus to ensure the removal of all volatile impurities using a Vacuubrand GMH-MD1 vacuum pump and an Edwards WRGS-NW35

turbomolecular pump to achieve ultra-high vacuum of 1×10^{-4} Pa. The apparatus can operate in the pressure range of (0.05 to 1.50) MPa using two pre-calibrated pressure controllers and in the temperature range from (293.15 to 773.15) K using a Polyscience SD07R-20 refrigerated recirculating water bath and a Severn TF50/3/12/F furnace. A Pt100 probe with a resolution of ± 0.01 K is located inside the reactor next to where the sample holder is suspended. Pressure was measured using a pressure transmitter with a resolution of $\pm 1 \times 10^{-6}$ MPa. Once loaded, the sample was degassed. Thereafter, the gas was introduced and controlled at the desired pressure and temperature. The low quantity of sample required and the programmable nature of the apparatus through the use of IGA software provided by Hiden Isochema Ltd., made absorption measurements efficient and less time consuming. Each data point took 1 to 4 hours to ensure equilibrium. Figure S-1 in supporting information illustrates the sample weight change with time for CO₂ in [MOA][Tf₂N] at 303.15 K and at 0.05 MPa, with that particular point taking approximately 1 hour for equilibrium due to small sample size and efficient temperature and pressure control. The absorption and desorption isotherms at 303.15, 313.15, 323.15 and 333.15 K were measured. Pressures of 0.050 – 1.500 MPa were considered in the case of CO₂, whilst in the case of O₂ it is 0.050 – 0.700 MPa due to limitations of gas regulation.

Due to the sample being of liquid form, there was a significant change in the sample density due to the absorption of the injected gas, thus making the sample more buoyant and altering the actual weight reading of the sample. The weight reading was hence not a true reflection of the actual mass of gas absorbed. To correct this, the buoyancy force was taken into account by first noting the weight reading of the sample at different gas pressures using a non-absorbent gas such as nitrogen or helium. The method of buoyancy correction is supplied as supporting information. Buoyancy correction is also explained in Macedonia et al.⁴⁸.

Absorption measurements were conducted and analysed with the data discussed in this study. Desorption measurements were also conducted however, to confirm the potential recyclability of the ionic liquids as solvents.

3. RESULTS AND DISCUSSION

The absorption and desorption of CO₂ and O₂ in [MOA][Tf₂N], [BMIM][Tf₂N] and [BMIM][MeSO₄] were determined by gravimetric analysis using an Intelligent Gravimetric Analyser (IGA). Systems with a fixed overall equilibrium composition of CO₂ and O₂ in [MOA][Tf₂N], [BMIM][Tf₂N] and [BMIM][MeSO₄] were measured as a function of temperature and pressure are given in Tables 2-7. Figures 3-8 graphically show CO₂ and O₂ absorption and desorption in [MOA][Tf₂N], [BMIM][Tf₂N] and [BMIM][MeSO₄] at different temperatures as a function of pressure. Desorption measurements showed no consistent pattern of being higher than absorption measurements. Hysteresis is minimal, indicating that CO₂ can be fully desorbed and recovered using these ionic liquids. From Figures 3-8, it can be seen that the absorption of both gases at all partial pressures was the highest at a lower temperature $T = 303.15$ K, and lowest at a higher temperature $T = 333.15$ K for each ionic liquid. This behaviour has also been observed in literature for other solvents including ionic liquids, confirming that absorption is an exothermic process.⁴⁹ Another observation of the absorption results, which is also consistent with literature^{5,7,22} is that an increase with gas partial pressure results in higher gas absorption for each ionic liquid. Additionally, the effect of cation and anion on absorption of gases in ionic liquids was studied and summarized in Figures 9 and 10, respectively.

Regarding the three ionic liquids studied in this work, two contain the same fluorinated anions [Tf₂N] but different class of cation such as [MOA], [BMIM] and two ionic liquids

have same cation [BMIM] but different anions of [Tf₂N] and [MeSO₄]. The molar masses are 648.85, 419.36 and 250.32 g·mol⁻¹ for [MOA][Tf₂N], [BMIM][Tf₂N] and [BMIM][MeSO₄], respectively. By using the density data, we calculated the molar volumes of these ionic liquids at $T = 303.15$ K and it was found that the molar volume decreases in the following order: [MOA][Tf₂N] (588.64 cm³·mol⁻¹) > [BMIM][Tf₂N] (292.87 cm³·mol⁻¹) > [BMIM][MeSO₄] (207.09 cm³·mol⁻¹). It is known that the absorption of gases in ionic liquids is mainly affected by two factors: (i) interaction between the gas and the anion of the ionic liquids and (ii) the molar volume of ionic liquids^{22,50}.

Regarding CO₂ absorption, Figures 3-5 show that [MOA][Tf₂N] achieved the highest CO₂ absorption at each temperature and partial pressures studied, followed by [BMIM][Tf₂N], with [BMIM][MeSO₄] achieving the lowest CO₂ absorption. This is because of the effect of cation, anion and molar volume of ionic liquids.

Figure 9 provides a further comparison of CO₂ absorption in the ionic liquids measured in this study to that of those measured in literature. It was found that CO₂ absorption in [MOA][Tf₂N] was higher than absorption in other ionic liquids such as [BMIM][PF₆] and also [HMIM][Tf₂N]. The [Tf₂N] anion is more highly fluorinated than the [PF₆] anion, and the [MOA] cation is larger than the [HMIM] cation. Further suggesting that CO₂ absorption is higher with increasing fluorination and cation chain length. It was also observed that [MOA][Tf₂N] achieved higher CO₂ absorption than [HMPY][Tf₂N] even when the CO₂ absorption in [HMPY][Tf₂N] was measured at lower temperature. This may either illustrate the effect of increasing cation chain length, or prove that ammonium based cations achieve superior CO₂ absorption over the imidazolium or pyridinium-based cations. CO₂ absorption was also higher in [MOA][Tf₂N] than in [BMPY][Tf₂N], at 333.15 K.

Figure 10 illustrates that [BMIM][Tf₂N] achieves higher CO₂ absorption than [HMPY][Tf₂N]. This is evident in that [BMIM][Tf₂N] achieves equal CO₂ absorption to that of [HMPY][Tf₂N] even though absorption in [BMIM][Tf₂N] was measured at a higher temperature. This suggests that imidazolium cations achieve higher CO₂ absorption than pyridinium cations. However, this is inconclusive since measurements at 333.15 K find similar CO₂ absorption achieved between [BMIM][Tf₂N] and [BMPY][Tf₂N]. Comparisons between measured and literature values at 323.15 K show CO₂ absorption to occur the highest in [HMIM][Tf₂N], followed by [BMIM][Tf₂N] and thereafter [BMIM][PF₆], confirming with good certainty that increased fluorination of the cation achieves increased CO₂ absorption and particular cation types, higher cation chain lengths increase CO₂ absorption. This confirms findings from other literature as well^{23,51} that a larger chain length of the cation in an IL results in higher absorption being achieved.

The effect of the anion on CO₂ absorption can be confirmed by also comparing the measured results between [BMIM][Tf₂N] and [BMIM][MeSO₄] seen in Figures 4 and 5, where [BMIM][Tf₂N] achieved higher CO₂ absorption than [BMIM][MeSO₄]. This is because [BMIM][Tf₂N] has a higher molar volume and greater interaction between CO₂ and [Tf₂N] than [MeSO₄] anion, due to increased fluorination.

As far as molar volume was concerned, it is proposed that ionic liquids with higher molar volume would achieve greater absorption of a gas solute.^{22,50,52-54} This may be because increasing the molar volume of ionic liquids increases the void space (free volume),^{55,45} and gases appear to be dissolved by occupying these free spaces available in ionic liquids.^{55,46,56}

It is clear from the result that the absorption of CO₂ in the tested ionic liquids decrease in order: [MOA][Tf₂N] > [BMIM][Tf₂N] > [BMIM][MeSO₄] being possible to achieve maximum mole fractions of absorbed CO₂ corresponding to 0.343, 0.283, and 0.138, respectively at $T = 303.15$ K and 1.5 MPa. The superior CO₂ absorption achieved by [MOA][Tf₂N] and [BMIM][Tf₂N] confirms that ionic liquids with fluorinated anions achieve higher CO₂ absorption than ionic liquids with non-fluorinated anions. The study also found that [MOA][Tf₂N] achieved higher CO₂ absorption at $T = 323.15$ K than more conventional ionic liquids such as [BMIM][BF₄] and [BMIM][PF₆] as measured by (Shiflett and Yokozeki)⁴⁹ and [HMIM][Tf₂N] by Anderson et al.,⁵⁰

Regarding O₂ absorption, Figure 7 shows a favourable comparison of measurements done in this work, with measurements conducted by Anthony et al (2005)²² at 323.15K. Data was especially comparable at low pressure while some deviation occurred at higher pressure of 0.7 MPa. This suggests that the technique of gravimetric analysis using N₂ for buoyancy correction may be accurate for systems O₂ especially at pressure below 0.4 MPa.

Figures 6-8, show that [MOA][Tf₂N] achieved the highest O₂ absorption at each temperature and partial pressure studied, followed by [BMIM][MeSO₄] with [BMIM][Tf₂N] achieving the lowest O₂ absorption. Figure 9 shows the effect of cation on O₂ absorption. From Figure 9 it can be seen that [MOA][Tf₂N] achieved the higher O₂ absorption than [BMIM][Tf₂N] due to the same effects that occurred for CO₂ absorption.

A short comparison with literature is illustrated in Figure 11. It can be observed that [MOA][Tf₂N] not only achieved the highest O₂ absorption of all ionic liquids in this work, but also achieved higher absorption than [BMPY][Tf₂N], measured by Anderson et al.⁵⁰. This

suggests that ammonium cations may be less CO₂ selective than imidazolium and pyridinium cations.

An observation of Figures 6 to 8 shows that [BMIM][MeSO₄] achieved higher O₂ absorption than [BMIM][Tf₂N]. These results show that the anions have a much larger effect on the O₂ absorption. The absorption of O₂ in ionic liquids decrease in order: [MOA][Tf₂N] > [BMIM][MeSO₄] > [BMIM][Tf₂N] being possible to achieve maximum mole fractions of absorbed/desorbed O₂ corresponding to 0.023, 0.013, and 0.006, respectively at $T = 303.15$ K and 0.7 MPa.

Furthermore, the ionic liquid [MOA][Tf₂N] achieved the highest CO₂ and O₂ absorption, indicating that this ionic liquid may not necessarily be favourable for gas separation processes appreciable amounts of both CO₂ and O₂, due to its low selectivity. By contrast, [BMIM][Tf₂N] achieved the 2nd highest CO₂ absorption capacity and the lowest O₂ absorption capacity, indicating that this ionic liquid is more selective towards CO₂ absorption and is hence more applicable in CO₂ capture processes.

An effective way of comparing ionic liquids and solvents for gas absorption is to calculate the Henry's law constant, K_H , of the absorbed gas in the binary system at each temperature.

$$K_{H \text{ gas,solvent } i, T} = \frac{P_{\text{gas}}}{x_{\text{gas}}} \quad (5)$$

where x_{gas} is the mole fraction of CO₂ and O₂ in IL and P_{gas} is the equilibrium pressure.

Table 8 contains Henry's law constant values measured in MPa for CO₂ and O₂ in all three ionic liquids and at each isotherm. A high deviation of 0.4 MPa is noted, due to higher Henry's law constants calculated at pressures of 1.3 and 1.5 MPa. . Nevertheless, a comparison of Henry's law constants confirms the conclusions drawn from the absorption measurements. The high selectivity of [BMIM][Tf₂N] for CO₂ absorption is ascertained by comparing the Henry's constants of CO₂ and O₂ for all isotherms.

Table 9 contains Enthalpy and Entropy of absorption for CO₂ and O₂ in all ionic liquids. Results for [BMIM][Tf₂N] compare favourably with Arshad (2009)³⁸. Enthalpy and Entropy of absorption values show that CO₂ absorption in [MOA][Tf₂N] is the least sensitive to temperature, while absorption in [BMIM][MeSO₄] is the most sensitive. The opposite is true in the case of O₂ absorption, although comparatively the high enthalpies and entropies of absorption for O₂ indicate low O₂ solubility in relation to CO₂ in these ionic liquids.

4. CORRELATION OF ABSORPTION DATA

The modelling of gas absorption in ionic liquids has been reported in numerous literature sources. More complex models take into account the asymmetry of cations and anions, as well as dipole and quadrupolar interactions.

Due to the relative simplicity of the ionic liquid species in this study in terms of asymmetry, absorption data of CO₂ and O₂ in all ionic liquids was successfully correlated using a much simpler equation of state (EOS). The generic RK-EOS was used, which was previously

applied successfully for ionic liquids containing fluorinated anions and imidazolium cations²³:

$$P = \frac{RT}{V - b} - \frac{a(T)}{V(V + b)} \quad (6)$$

where $a(T)$ in eq 6, is a function of temperature and species mole fraction. For the components in this work, the Van der Waals-Berthelot mixing formula was used as successfully applied for similar systems.^{23,57}

$$a(T) = \sum_{i,j=1}^N \sqrt{a_i a_j} \left(1 + \frac{\tau_{ij}}{T} \right) (1 - k_{ij}) x_i x_j \quad \text{where } k_{ij} = \frac{l_{ij} l_{ji} (x_i + x_j)}{l_{ji} x_i + l_{ij} x_j} \quad (7)$$

$$a_i = 0.427480 \frac{R^2 T_{ci}^2}{P_{ci}} \alpha_i(T) \quad \text{where } \alpha_i(T) = \sum_{k=0}^{\leq 3} \beta_k \left(\frac{T_c}{T} - \frac{T}{T_c} \right)^k \quad (8)$$

$$\text{and } b = \frac{1}{2} \sum_{i,j=1}^N (b_i + b_j) (1 - m_{ij}) (1 - k_{ij}) x_i x_j \quad \text{where } b_i = 0.08664 \frac{RT_{ci}}{P_{ci}} \quad (9)$$

l_{ij} , l_{ji} , k_{ij} , and m_{ij} are binary interaction parameters with $m_{ij} = m_{ji}$ and $m_{ii} = 0$. Coefficients β_k are treated as adjustable fitting parameters. As with many other ionic liquids, critical temperature and pressure could not be found in literature for the ionic liquids in this study. This is due to ionic liquids decomposing before reaching their critical point.

Critical temperature and pressure were thus computed using a modified Lydersen-Joback-Reid group contribution method:^{58,59}

$$T_c = \frac{T_b}{A_M + B_M \sum n \Delta T_M - \left(\sum n \Delta T_M \right)^2} \quad \text{where } T_b = 198.2 + \sum n \Delta T_{bM} \quad (10)$$

$$P_c = \frac{M}{\left[C_M + \sum n \Delta P_M \right]^2} \quad (11)$$

where $A_M = 0.5703$, $B_M = 1.0121$, $C_M = 0.2573$, $E_M = 6.75$. n is the number of occurrences of any particular functional group in the molecule. Group contributions of ΔT_{bM} are provided in the work of Alvarez and Valderrama.⁵⁸

In this study, we modelled the absorption of CO₂ and O₂ in all three ionic liquids. Model parameters are provided as supporting information in Table S1 while estimated critical properties are shown in Table S2.

Figures 3 - 8, illustrate the model-calculated CO₂ and O₂ partial pressure using parameters obtained by data regression, in comparison to the measured data. It is evident that model estimates compare quite favourably with measured data. The root-mean-square error for each system is provided in Table 9, showing very good accuracy of model estimates, which is consistent with the work of Shiflett and Yokozeki⁴⁹ for CO₂ absorption in [BMIM][PF₆] and [BMIM][BF₄].

It is observed from Figures 6 - 8 that O₂ absorption decreases significantly with increasing temperature. The temperature effect is far more pronounced than with CO₂ absorption. As a result modelling of the data became more difficult, and while Table 9 contains regressed parameters for CO₂ absorption in all ionic liquids, common for all temperatures, parameters for O₂ absorption differ for each isotherm.

5. CONCLUSIONS

Absorption measurements of CO₂ and O₂ in the ionic liquids [MOA][Tf₂N], [BMIM][Tf₂N] and [BMIM][MeSO₄] have been reported. The data of each isotherm was confirmed to incur low hysteresis. The ionic liquid [MOA][Tf₂N] achieved the highest CO₂ and O₂ absorption from all the ionic liquids studied and some other ionic liquids compared in the literature, which indicates good CO₂ solubility but undesirably low CO₂ selectivity. The ionic liquid [BMIM][Tf₂N], although having not achieved the highest CO₂ absorption of the three ionic liquids studied, was found the most suitable for CO₂ absorption from flue gas due to its higher selectivity of CO₂ over O₂. The calculation of Henry's law constants for CO₂ and O₂ in all ionic liquids at all isotherms confirmed the findings made by analysis of the absorption data, and provide an effective numerical comparison of ionic liquids performance as gas absorbents. A further analysis of enthalpy and entropy of absorption revealed solubility in [BMIM][MeSO₄] to be highly temperature sensitive. The generic RK-EOS model achieved accurate estimates for all systems studied, with a root mean square error of no higher than 1.98 kPa. The model was found to be more robust for systems containing CO₂, while parameter regression became more temperature sensitive with systems containing O₂.

AUTHOR INFORMATION

Corresponding Author

*E-mail: ramjuger@ukzn.ac.za (D. Ramjugernath). Tel.: +27 (31) 2603128. Fax: +27 (31) 2601118.

Notes

The authors declare no competing financial interest.

ACKNOWLEDGMENTS

The authors acknowledge University of KwaZulu-Natal for a doctoral scholarship for Mr K. Osman and postdoctoral scholarship for Dr I. Bahadur. This work is based upon research supported by the South African Research Chairs Initiative of the Department of Science and Technology and the National Research Foundation.

REFERENCES

- (1) Bretherick, L. ed. Hazards in the Chemical Laboratory, 6th edition. *Royal Society of Chemistry*, Cambridge, UK, **1994**.

- (2) Valavavanidis, A.; Basic Principles of Health and Safety in Chemical and Biochemical Laboratories. Information for toxic substances. Department of Chemistry, University of Athens, Athens, **2006** (www.chem.uoa.gr).
- (3) IPCC. In *Climate Change 2007: The Physical Science Basis. Contribution of Working Group I to the Fourth Assessment Report of the Intergovernmental Panel on Climate Change*; Cambridge University Press: Cambridge, U.K., and New York, **2007**.
- (4) Govinda, V.; Reddy, P. M.; Bahadur, I.; Attri, P.; Venkatesu, P.; Venkateswarlu, P. Effect of anion variation on the thermophysical properties of triethylammonium based protic ionic liquids with polar solvent. *Thermochim. Acta* **2013**, *556*, 75–88.
- (5) Tang, S.; Baker, G. A.; Zhao, H. Ether- and alcohol-functionalized task-specific ionic liquids: attractive properties and applications. *Chem. Soc. Rev.* **2012**, *41*, 4030–4066.
- (6) Davis, J. H. Task-specific ionic liquids, *Chem. Lett.* **2004**, *33*, 1072–1077.
- (7) Rodríguez, H.; Brennecke, J. F. Temperature and composition dependence of the density and viscosity of binary mixtures of water + ionic liquid. *J. Chem. Eng. Data* **2006**, *51*, 2145–2155.
- (8) Deenadayalu, N.; Bahadur, I.; Hofman, T. Ternary excess molar volumes of {methyltrioctylammonium bis(trifluoromethylsulfonyl)imide + ethanol + methyl acetate, or ethyl acetate} systems at $T = (298.15, 303.15, \text{ and } 313.15) \text{ K}$. *J. Chem. Thermodyn.* **2010**, *42*, 726–733.
- (9) Bahadur, I.; Deenadayalu, N. Apparent Molar Volume and Isentropic Compressibility for the Binary Systems {Methyltrioctylammonium Bis(trifluoromethylsulfonyl)imide + Methyl Acetate or Methanol} and (Methanol + Methyl Acetate) at $T = 298.15, 303.15, 308.15 \text{ and } 313.15 \text{ K}$ and Atmospheric Pressure. *J Solution Chem.* **2011**, *40*, 1528–1543.

- (10) Bahadur, I.; Deenadayalu, N. Apparent Molar Volume and Apparent Molar Isentropic Compressibility for the Binary Systems {Methyltrioctylammonium bis(trifluoromethylsulfonyl)imide + Ethyl Acetate or Ethanol} at Different Temperatures under Atmospheric Pressure. *Thermochim. Acta* **2013**, *566*, 77–83.
- (11) Deenadayalu, N.; Bahadur, I.; Hofman, T. Ternary Excess Molar Volumes of {Methyltrioctylammonium Bis[(trifluoromethyl)sulfonyl]imide + Methanol + Methyl Acetate or Ethyl Acetate} Systems at (298.15, 303.15, and 313.15) K. *J. Chem. Eng. Data* **2010**, *55*, 2636–2642.
- (12) Wood, N.; Stephens, G. Accelerating the discovery of biocompatible ionic liquids. *Phys. Chem. Chem. Phys.* **2010**, *12*, 1670–1674.
- (13) Bahadur, I.; Deenadayalu, N.; Tywabi, Z.; Sen, S.; Hofman, T. Volumetric properties of ternary (IL + 2-propanol or 1-butanol or 2-butanol + ethyl acetate) systems and binary (IL + 2-propanol or 1-butanol or 2-butanol) and (1-butanol or 2-butanol + ethyl acetate) systems. *J. Chem. Thermodyn.* **2012**, *49*, 24–38.
- (14) Dreisbach, F.; Meister, D.; Lösch, H. W.; Weißert, T.; Petermann, M. Ionic liquids for gas separation: Measurement of selective gas solubilities of the gas-mixture CH₄/CO₂. http://www.merrowscientific.com/Portals/55675/docs/Ionic_Liquids.pdf **2013**.
- (15) Wasserscheid, P.; Welton, T. Ionic Liquids in Synthesis. *Wiley-VCH: Weinheim, Germany*, **2003**.
- (16) Plechkova, N. V.; Seddon, K. R. Applications of Ionic Liquids in the Chemical Industry. *Chem. Soc. Rev.* **2008**, *37*, 123–150.
- (17) Palomar, J.; Torrecilla, J. S.; Ferro, V.; Rodriguez, F. Development of an a Priori Ionic Liquid Design Tool. 1. Integration of a Novel COSMO-RS Molecular Descriptor on Neural Networks. *Ind. Eng. Chem. Res.* **2008**, *47*, 4523–4532.

- (18) Palomar, J.; Torrecilla, J. S.; Ferro, V.; Rodriguez, F. Development of an a Priori Ionic Liquid Design Tool. 2. Ionic Liquid Selection through the Prediction of COSMO-RS Molecular Descriptor by Inverse Neural Network. *Ind. Eng. Chem. Res.* **2009**, *48*, 2257–2265.
- (19) Holbrey, J. D.; Seddon, K. R. Ionic Liquids. *Clean Products Processes* **1999**, *1*, 223–236.
- (20) Welton, T. Room-Temperature Ionic Liquids. Solvents for Synthesis and Catalysis. *Chem. Rev.* **1999**, *99*, 2071–2083.
- (21) Wasserscheid, P.; Keim, W. Ionic liquid-new “solution” for transition metal catalysis. *Angew. Chem., Int. Ed. Engl.* **2000**, *39*, 3773–3789.
- (22) Anthony, J. L.; Anderson, J. L.; Maginn, E. J.; Brennecke, J. F. Anion Effects on Gas Solubility in Ionic Liquids. *J. Phys. Chem. B* **2005**, *109*, 6366–6374.
- (23) Shiflett, M. B.; Yokozeki, A. Solubility of CO₂ in Room Temperature Ionic Liquid [hmim][Tf₂N]. *J. Phys. Chem. B* **2007**, *111*, 2070–2074.
- (24) Almantariotis, D.; Stevanovic, S.; Fandiño, O.; Pensado, A. S.; Padua, A. A. H.; Coxam, J.-Y.; Gomes, M. F. C. Absorption of Carbon Dioxide, Nitrous Oxide, Ethane and Nitrogen by 1-Alkyl-3-methylimidazolium (C_nmim, *n* = 2, 4, 6) Tris (pentafluoroethyl) trifluorophosphate Ionic Liquids (eFAP). *J. Phys. Chem. B* **2012**, *116*, 7728–7738.
- (25) Gonzalez-Miquel, M.; Bedia, J.; Abrusci, C.; Palomar, J.; Rodríguez, F. Anion Effects on Kinetics and Thermodynamics of CO₂ Absorption in Ionic Liquids. *J. Phys. Chem. B* **2013**, *117*, 3398–3406.
- (26) Kumelan, J.; Kamps, Ä. P.-S.; Tuma, D.; Yokozeki, A.; Shiflett, M. B.; Maurer, G. Solubility of Tetrafluoromethane in the Ionic Liquid [hmim][Tf₂N]. *J. Phys. Chem. B* **2008**, *112*, 3040–3047.

- (27) Zhou, L.; Fan, J.; Shang, X.; Wang, J. Solubilities of CO₂, H₂, N₂ and O₂ in ionic liquid 1-*n*-butyl-3-methylimidazolium Heptafluorobutyrate. *J. Chem. Thermodyn.* **2013**, *59*, 28–34.
- (28) Afzal, W.; Liu, X.; Prausnitz, J. M. Solubilities of some gases in four imidazolium-based ionic liquids. *J. Chem. Thermodyn.* **2013**, *63*, 88–94.
- (29) Oh, D.-J.; Lee, B.-C. High-pressure phase behavior of carbon dioxide in ionic liquid 1-butyl-3-methylimidazolium bis(trifluoromethylsulfonyl)imide. *Korean J. Chem. Eng.* **2006**, *23*, 800–805.
- (30) Sa´nchez, L. M. G.; Meindersma, G. W.; De Haan, A. B. Solvent properties of functionalized ionic liquids for CO₂ absorption. *Chem. Eng. Res. Des.* **2007**, *85*, 31–39.
- (31) Raeissi, S.; Florusse, L. J.; Peters, C. J. Hydrogen Solubilities in the IUPAC Ionic Liquid 1-Hexyl-3-methylimidazolium Bis(Trifluoromethylsulfonyl)Imide. *J. Chem. Eng. Data* **2011**, *56*, 1105–1107.
- (32) Ren, S.; Hou, Y.; Tian, S.; Chen, X.; Wu, W. What Are Functional Ionic Liquids for the Absorption of Acidic Gases?. *J. Phys. Chem. B* **2013**, *117*, 2482–2486.
- (33) Jacquemin, J.; Husson, P.; Padua, A. A. H.; Majer, V. Density and viscosity of several pure and water-saturated ionic liquids. *Green Chem.* **2006**, *8*, 172–180.
- (34) Muldoon M.J., Aki S.N.V.K., Anderson J.L., Dixon J.K., and Brennecke J.F., Improving Carbon Dioxide Solubility in Ionic Liquids, *J. Phys. Chem. B* **2007**, *111*, 9001-9009
- (35) Palgunadi J., Kang J.E., Cheong M., Kim H., Lee H., and Kim H.S., Fluorine-free imidazolium-based ionic liquids with a phosphorous-containing anion as potential CO₂ absorbents, *Bull. Korean Chem. Soc., Vol. 30* **2009**, pg. 1749-1754.

- (36) Pereiro, A. B.; Verdr'a, P.; Tojo, E.; Rodr'iguez, A. Physical Properties of 1-Butyl-3-methylimidazolium Methyl Sulfate as a Function of Temperature. *J. Chem. Eng. Data* **2007**, *52*, 377–380.
- (37) Zhang Y., Zhang S., Lu X., Zhou Q., Fan W., and Zhang X., Dual amino-functionalised phosphonium ionic liquids for CO₂ capture”, *Chem. Eur. J., Vol. 15* **2009**, pg. 3003-3011.
- (38) Arshad M.W., CO₂ capture using Ionic Liquids, Department of Chemical and Biochemical Engineering, Technical University of Denmark, 2009. Accessed 28/3/2011.
- (39) Hasib-ur-Rahman M., Siaj M., Larachi F., Ionic liquids for CO₂ capture—Development and progress, *Chem. Eng. Proc. Vol. 49* **2010**, Pg. 313–322.
- (40) SuoJiang Z., XiangPing Z., YanSong Z., GuoYing Z., XiaoQian Y., and HongWei Y., A novel ionic liquids-based scrubbing process for efficient CO₂ capture”, *Science China Chemistry Vol.53*, **2010**, Pg. 1549-1553.
- (41) Cadena C., Anthony J.L., Shah J.K., Morrow T.I., Brennecke J.F., and Maginn E.J., Why Is CO₂ So Soluble in Imidazolium-Based Ionic Liquids?”, *J. Am. Chem. Soc., vol. 126* **2004**, pg. 5300-5308
- (42) Huang J. and R'uther T., Why are ionic liquids attractive for CO₂ absorption? An overview, *Aust. J. Chem., vol. 62* **2009**, pg. 298-308.
- (43) Baltus R.E., Culbertson B.H., Dai S., Luo H., and DePaoli D.W., Low-pressure solubility of carbon dioxide in room-temperature ionic liquids measured with a quartz crystal microbalance, *J. Phys. Chem. B, Vol. 108*, **2004**, pg. 721-727.
- (44) Brennecke J.F. and Gurkan B.E., Ionic liquids for CO₂ capture and emission reduction, *J. Phys. Chem. Lett., Vol. 1*, **2010**, Pg.3459–3464.

- (45) Shannon, M. S.; Tedstone, J. M.; Danielsen, S. P. O.; Hindman, M.S.; Irvin, A. C.; Bara, J. E. Fractional Free Volume as the Basis of Gas Solubility & Selectivity in Imidazolium-based Ionic Liquids. *Ind. Eng. Chem. Res.* **2012**, *51*, 5565–5576.
- (46) Scovazzo, P.; Camper, D.; Kieft, J.; Poshusta, J.; Koval, C.; Noble, R. D. Regular solution theory and CO₂ gas solubility in room temperature ionic liquids. *Ind. Eng. Chem. Res.* **2004**, *43*, 6855–6860.
- (47) Kumelan J., Tuma D., Kamps A.P.S., and Maurer G., Solubility of the Single Gases Carbon Dioxide and Hydrogen in the Ionic Liquid [bmpy][Tf2N], *J. Chem. Eng. Data* **2010**, *55*, 165–172
- (48) Macedonia, M. D.; Moore, D. D.; Maginn, E. J. Adsorption Studies of Methane, Ethane, and Argon in the Zeolite Mordenite: Molecular Simulations and Experiments. *Langmuir* **2000**, *16*, 3823–3834.
- (49) Shiflett, M. B.; Yokozeki, A. Solubilities and diffusivities of carbon dioxide in ionic liquids: [bmim][PF₆] and [bmim][BF₄]. *Ind. Eng. Chem. Res.* **2005**, *44*, 4453–4464.
- (50) Zhou, L.; Fan, J.; Shang, X.; Wang, J. Solubilities of CO₂, H₂, N₂ and O₂ in ionic liquid 1-*n*-butyl-3-methylimidazolium heptafluorobutyrate. *J. Chem. Thermodyn.* **2013**, *59*, 28–34.
- (51) Anderson, J. L.; Dixon, J. K.; Brennecke, J. F. Solubility of CO₂, CH₄, C₂H₆, C₂H₄, O₂, and N₂ in 1-hexyl-3-methylpyridinium bis(trifluoromethylsulfonyl)imide: Comparison to other ionic liquids. *Acc. Chem. Res.* **2007**, *40*, 1208–1216.
- (52) Seki, T.; Grunwaldt, J.-D.; Baiker, A. In Situ Attenuated Total Reflection Infrared Spectroscopy of Imidazolium-Based Room-Temperature Ionic Liquids under “Supercritical” CO₂. *J. Phys. Chem. B* **2009**, *113*, 114–122.

(53) Kazarian, S. G.; Briscoe, B. J.; Welton, T. Combining ionic liquids and supercritical fluids: in situ ATR-IR study of CO₂ dissolved in two ionic liquids at high pressures.

Chem. Commun. **2000**, 2047–2048.

(54) Camper, D.; Bara, J. E.; Koval, C.; Noble, R. D. Gas solubilities in room-temperature ionic liquids. *Ind. Eng. Chem. Res.* **2006**, *45*, 6279–6283.

(55) Finotello, A.; Bara, J. E.; Narayan, S.; Camper, D.; Noble, R. D. Ideal Gas Solubilities and Solubility Selectivities in a Binary Mixture of Room-Temperature Ionic Liquids. *J. Phys. Chem. B* **2008**, *112*, 2335–2339.

(56) Huang, X.; Margulis, C. J.; Li, Y.; Berne, B. J. Why is the Partial Molar Volume of CO₂ So Small When Dissolved in a Room Temperature Ionic Liquid? Structure and Dynamics of CO₂ Dissolved in [Bmim]⁺[PF₆]⁻. *J. Am. Chem. Soc.* **2005**, *127*, 17842–17851.

(57) Yokozeki, A. Solubility of refrigerants in various lubricants. *Int. J. Thermophys.* **2001**, *22*, 1057–1071.

(58) Alvarez, V. H.; Valderrama, J. O. A modified Lydersen-Joback-Reid method to estimate the critical properties of biomolecules. *Alimentaria* **2004**, *254*, 55–66.

(59) Valderrama, J. O.; Robles, P. A. Critical properties, normal boiling temperatures, and acentric factors of fifty ionic liquids. *Ind. Eng. Chem. Res.* **2007**, *46*, 1338–1344.

Table 1: Densities, ρ , and Refractive Index, n , of Pure ILs together with Literatures at Experimental Temperature

Component	T/K	$\rho/(\text{g}\cdot\text{cm}^{-3})$		n	
		Exp.	Lit.	Exp.	Lit.
[MOA][Tf ₂ N]	303.15	1.10228	1.1032 ^a	1.43656	-
	313.15	1.09474	1.0957 ^a	1.43341	-
	323.15	1.08720	-	1.43035	-
	333.15	1.07970	-	1.42721	-
[BMIM][Tf ₂ N]	303.15	1.43191	1.4334 ^b	1.42546	-
	313.15	1.42233	1.4239 ^b	1.42251	-
	323.15	1.41283	1.4144 ^b	1.41945	-
	333.15	1.40338	1.4048 ^b	1.41655	-
[BMIM][MeSO ₄]	303.15	1.20873	1.20881 ^c	1.47809	1.47805 ^c
	313.15	1.20198	1.20204 ^c	1.47532	1.47536 ^c
	323.15	1.19606	1.19534 ^c	1.47261	1.47266 ^c
	333.15	1.18845	1.18873 ^c	1.46998	1.47000 ^c

^aFrom ref 8. ^bFrom ref 33. ^cFrom ref 36.

Table 2: Experimental Results for Absorption and Desorption of CO₂ in [MOA][Tf₂N]

$P_{\text{meas}}/\text{MPa}$	T/K	x_{CO_2}	$P_{\text{meas}}/\text{MPa}$	T/K	x_{CO_2}	$P_{\text{calc}}/\text{MPa}$
	absorption			desorption		
0.0499	303.18	0.017	0.0499	303.17	0.017	0.0500
0.1000	303.21	0.031	0.0998	303.15	0.035	0.1000
0.3998	303.18	0.122	0.3998	303.21	0.138	0.4003
0.7000	303.18	0.198	0.7000	303.15	0.197	0.7005
1.0000	303.18	0.263	0.9998	303.05	0.280	1.0000
1.2999	303.17	0.319	1.2997	303.17	0.323	1.3000
1.4999	303.23	0.343	1.4999	303.23	0.344	1.5011
0.0499	313.25	0.019	0.0500	313.14	0.013	0.0500
0.1000	313.09	0.027	0.0998	313.13	0.030	0.0999
0.4000	313.13	0.104	0.3998	313.07	0.110	0.3999
0.6999	313.15	0.173	0.7000	313.10	0.187	0.6999
0.9997	313.13	0.235	0.9999	313.12	0.235	0.9993
1.2999	313.16	0.287	1.2998	313.07	0.293	1.2989
1.4996	313.17	0.313	1.4996	313.17	0.314	1.4992
0.0500	323.26	0.0143	0.0499	323.16	0.010	0.0500
0.1000	323.18	0.0215	0.0998	323.10	0.022	0.0999
0.4001	323.14	0.0886	0.3998	323.22	0.094	0.3997
0.7000	323.20	0.1511	0.6999	323.07	0.154	0.6999
0.9999	323.19	0.1981	1.0000	323.19	0.212	0.9999
1.3000	323.17	0.2493	1.3000	323.05	0.260	1.2993
1.5000	323.15	0.2820	1.5000	323.15	0.282	1.4992
0.0500	333.24	0.0112	0.0499	333.14	0.006	0.0500
0.0999	333.14	0.0178	0.0999	333.24	0.017	0.0999
0.3999	333.12	0.0773	0.3998	333.18	0.086	0.3996
0.6998	333.11	0.1330	0.6999	333.04	0.141	0.6999
1.0000	333.24	0.1802	0.9999	333.07	0.191	1.0006
1.2998	333.16	0.2281	1.2998	333.12	0.234	1.3005
1.4999	333.13	0.2595	1.4999	333.13	0.258	1.5006

Uncertainty: $T = \pm 0.01$ K; $P = 1 \times 10^{-6}$ MPa; $x = \pm 0.00005$

Table 3: Experimental Results for Absorption and Desorption of CO₂ in BMIM][Tf₂N]

$P_{\text{meas}}/\text{MPa}$	T/K	x_{CO_2}	$P_{\text{meas}}/\text{MPa}$	T/K	x_{CO_2}	$P_{\text{calc}}/\text{MPa}$
absorption			desorption			
0.0499	303.22	0.016	0.0499	303.17	0.014	0.0504
0.1000	303.16	0.027	0.0999	303.13	0.028	0.0996
0.4000	303.18	0.096	0.3998	303.14	0.104	0.3996
0.7000	303.18	0.158	0.6994	303.06	0.165	0.7000
0.9998	303.25	0.202	0.9996	303.06	0.219	1.0009
1.3001	303.20	0.260	1.2996	303.10	0.263	1.3013
1.4999	303.22	0.283	1.4999	303.22	0.282	1.5021
0.0499	313.28	0.015	0.0499	313.17	0.008	0.0503
0.1000	313.19	0.020	0.0998	313.15	0.024	0.0984
0.4001	313.13	0.077	0.3998	313.10	0.083	0.3993
0.7001	313.18	0.131	0.6997	313.05	0.135	0.6996
1.0001	313.14	0.178	0.9995	313.07	0.182	0.9996
1.2998	313.14	0.216	1.2999	313.12	0.223	1.299
1.5000	313.11	0.245	1.5000	313.11	0.245	1.4977
0.0500	323.27	0.011	0.0499	323.15	0.005	0.0501
0.1000	323.22	0.016	0.0998	323.15	0.013	0.1019
0.3999	323.20	0.064	0.3997	323.09	0.051	0.3992
0.7000	323.14	0.108	0.6998	323.12	0.098	0.6994
1.0000	323.24	0.147	0.9997	323.17	0.140	1.0000
1.3000	323.09	0.186	1.2999	323.10	0.179	1.2985
1.5000	323.17	0.210	1.5000	323.17	0.210	1.4974
0.0498	333.18	0.004	0.0499	333.07	0.005	0.0501
0.0999	333.15	0.010	0.1000	333.06	0.010	0.1005
0.4020	333.21	0.042	0.3999	333.22	0.052	0.3982
0.7001	333.21	0.094	0.6999	333.14	0.091	0.6995
0.9998	333.17	0.119	0.9998	333.17	0.124	1.0003
1.3000	333.19	0.145	1.2999	333.12	0.141	1.3015
1.5000	333.17	0.155	1.5001	333.14	0.149	1.5028

Uncertainty: $T = \pm 0.01$ K; $P = 1 \times 10^{-6}$ MPa; $x = \pm 0.00005$

Table 4: Experimental Results for Absorption and Desorption of CO₂ in [BMIM][MeSO₄]

$P_{\text{meas}}/\text{MPa}$	T/K	x_{CO_2}	$P_{\text{meas}}/\text{MPa}$	T/K	x_{CO_2}	$P_{\text{calc}}/\text{MPa}$
absorption			desorption			
0.0499	303.18	0.005	0.0505	303.18	0.008	0.0500
0.1000	303.20	0.010	0.1001	303.19	0.015	0.1000
0.3997	303.16	0.045	0.4011	303.16	0.048	0.4000
0.7001	303.09	0.084	0.7003	303.09	0.085	0.6998
1.0001	303.20	0.104	0.9996	303.10	0.106	1.0006
1.3001	303.17	0.130	1.3001	303.09	0.132	1.3003
1.5000	303.17	0.138	1.5000	303.17	0.140	1.5012
0.0506	313.25	0.008	0.0509	313.15	0.007	0.0500
0.0998	313.20	0.010	0.1005	313.14	0.013	0.1000
0.4005	313.13	0.038	0.4000	313.06	0.040	0.3998
0.6998	313.11	0.074	0.6999	313.17	0.071	0.6994
1.0000	313.14	0.096	0.9995	313.05	0.097	0.9994
1.3000	313.16	0.118	1.2999	313.11	0.117	1.2989
1.5000	313.16	0.129	1.5000	313.16	0.129	1.4988
0.0507	323.23	0.007	0.0502	323.14	0.003	0.0500
0.1003	323.11	0.007	0.1004	323.11	0.007	0.1000
0.4000	323.15	0.035	0.4004	323.19	0.035	0.3997
0.7001	323.19	0.058	0.7001	323.08	0.058	0.6998
1.0001	323.24	0.078	1.0001	323.15	0.077	1.0001
1.2999	323.23	0.097	1.3000	323.21	0.099	1.3004
1.4999	323.13	0.112	1.4999	323.13	0.109	1.4991
0.0504	333.23	0.003	0.0506	333.04	-0.001	0.0500
0.1011	333.10	0.004	0.1004	333.10	0.003	0.1000
0.3998	333.22	0.028	0.4000	333.20	0.030	0.3998
0.6999	333.25	0.047	0.7000	333.17	0.050	0.6999
0.9998	333.09	0.065	0.9998	333.07	0.069	0.9998
1.2998	333.13	0.083	1.3000	333.08	0.085	1.3004
1.5000	333.05	0.092	1.5000	333.05	0.092	1.5009

Uncertainty: $T = \pm 0.01 \text{ K}$; $P = 1 \times 10^{-6} \text{ MPa}$; $x = \pm 0.00005$

Table 5: Experimental Results for Absorption and Desorption of O₂ in [MOA][Tf₂N]

$P_{\text{meas}}/\text{MPa}$	T/K	x_{O_2}	$P_{\text{meas}}/\text{MPa}$	T/K	x_{O_2}	$P_{\text{calc}}/\text{MPa}$
	absorption			desorption		
0.0499	303.11	0.004	0.0498	303.17	0.003	0.0499
0.0999	303.19	0.008	0.0999	303.11	0.008	0.0999
0.3997	303.15	0.016	0.3997	303.11	0.016	0.3997
0.6998	303.15	0.023	0.6998	303.15	0.024	0.6998
0.0498	313.31	0.002	0.0498	313.14	0.001	0.0511
0.0999	313.11	0.004	0.0999	313.10	0.002	0.1012
0.3997	313.21	0.013	0.3998	313.07	0.012	0.3996
0.7000	313.17	0.020	0.7000	313.17	0.021	0.7000
0.0498	323.25	0.000	0.0498	323.13	0.000	0.0499
0.0999	323.18	0.001	0.0999	323.23	0.002	0.0999
0.3999	323.24	0.008	0.3998	323.16	0.007	0.3999
0.6999	323.15	0.013	0.6999	323.15	0.013	0.6999
0.0498	333.28	0.000	0.0498	333.15	0.0002	0.0497
0.0999	333.18	0.001	0.0999	333.11	0.0003	0.0994
0.3996	333.23	0.003	0.3997	333.25	0.003	0.3996
0.7000	333.05	0.004	0.7000	333.05	0.003	0.7000

Uncertainty: $T = \pm 0.01$ K; $P = 1 \times 10^{-6}$ MPa; $x = \pm 0.00005$

Table 6: Experimental Results for Absorption and Desorption of O₂ in [BMIM][Tf₂N]

$P_{\text{meas}}/\text{MPa}$	T/K	x_{O_2}	$P_{\text{meas}}/\text{MPa}$	T/K	x_{O_2}	$P_{\text{calc}}/\text{MPa}$
absorption			desorption			
0.0498	303.19	0.001	0.050	303.162	0.001	0.0500
0.0999	303.17	0.002	0.100	303.071	0.002	0.0999
0.3999	303.22	0.006	0.400	303.109	0.005	0.3999
0.7000	303.25	0.006	0.700	303.248	0.005	0.7000
0.0498	313.29	0.001	0.050	313.154	0.001	0.0500
0.0999	313.12	0.002	0.100	313.059	0.001	0.0999
0.3999	313.12	0.004	0.400	313.054	0.004	0.3999
0.7001	313.20	0.005	0.700	313.197	0.005	0.7001
0.0499	323.27	0.000	0.050	323.143	0.001	0.0500
0.0998	323.09	0.001	0.100	323.220	0.001	0.0999
0.3998	323.24	0.003	0.400	323.138	0.003	0.3998
0.6999	323.23	0.005	0.700	323.234	0.004	0.6999
0.0500	333.29	0.0003	0.050	333.138	0.0003	0.0500
0.0999	333.19	0.0003	0.100	333.114	0.0002	0.0999
0.3999	333.15	0.0004	0.400	333.066	0.0003	0.3999
0.7000	333.19	0.0005	0.700	333.186	0.0005	0.6999

Uncertainty: $T = \pm 0.01$ K; $P = 1 \times 10^{-6}$ MPa; $x = \pm 0.00005$

Table 7: Experimental Results for Absorption and Desorption of O₂ in [BMIM][MeSO₄]

$P_{\text{meas}}/\text{MPa}$	T/K	x_{O_2}	$P_{\text{meas}}/\text{MPa}$	T/K	x_{O_2}	$P_{\text{calc}}/\text{MPa}$
absorption			desorption			
0.0495	303.18	0.007	0.0495	303.19	0.007	0.0500
0.0994	303.15	0.008	0.0996	303.06	0.008	0.0999
0.3994	303.22	0.012	0.3994	303.11	0.012	0.3989
0.6995	303.06	0.013	0.6995	303.06	0.013	0.6997
0.0496	313.30	0.007	0.0495	313.14	0.007	0.0486
0.0994	313.15	0.007	0.0996	313.06	0.007	0.0973
0.3995	313.08	0.011	0.3995	313.04	0.011	0.3942
0.6995	313.15	0.012	0.6995	313.15	0.012	0.7000
0.0495	323.33	0.006	0.0496	323.14	0.005	0.0496
0.0993	323.11	0.007	0.0996	323.16	0.007	0.0999
0.3993	323.20	0.009	0.3996	323.17	0.009	0.3992
0.6995	323.23	0.010	0.6995	323.23	0.010	0.6995
0.0495	333.35	0.003	0.0497	333.13	0.003	0.0501
0.0998	333.10	0.003	0.0995	333.13	0.003	0.0999
0.3993	333.10	0.005	0.3996	333.24	0.005	0.3993
0.6996	333.15	0.007	0.6996	333.15	0.007	0.6996

Uncertainty: $T = \pm 0.01 \text{ K}$; $P = 1 \times 10^{-6} \text{ MPa}$; $x = \pm 0.00005$

Table 8: Henry's Law Constants of CO₂ and O₂ (K_{HCO_2} and K_{HO_2}) in [MOA][Tf₂N], [BMIM][Tf₂N] and [BMIM][MeSO₄] Estimated from Absorption Data

T/K	[MOA][Tf ₂ N]	[BMIM][Tf ₂ N]	[BMIM][MeSO ₄]
	$K_{\text{HCO}_2}/\text{MPa}$		
303.15	3.7	4.6	9.6
313.15	4.2	5.6	10.5
323.15	4.9	6.7	12.9
333.15	5.5	9.0	15.3
	$K_{\text{HO}_2}/\text{MPa}$		
303.15	19.6	65.6	26.6
313.15	30.9	82.9	28.9
323.15	59.1	128.6	36.1
333.15	138.1	223.7	58.9

Table 9: Enthalpy and Entropy of Absorption for CO₂ and O₂ in the Ionic Liquids Studied in this Work

	[BMIM][Tf ₂ N]	[MOA][Tf ₂ N]	[BMIM][MeSO ₄]
	$\Delta H/\text{kJ}\cdot\text{mol}^{-1}$		
CO ₂	-13.46 ± 1.8	-10.46 ± 1.8	-18.15 ± 4.46
O ₂	-26.80 ± 2.32	-25.53 ± 3.45	-9.25 ± 3.29
	$\Delta S/\text{J}\cdot\text{mol}^{-1}\cdot\text{K}^{-1}$		
CO ₂	-45.30 ± 5.74	-34.27 ± 4.96	-47.52 ± 5.47
O ₂	-79.12 ± 19.07	-81.80 ± 11.02	-35.62 ± 2.61

Figure Captions

Figure 1. 3D structure of ionic liquids: (a) [MOA][Tf₂N], (b) [BMIM][Tf₂N] and (c) [BMIM][MeSO₄] used in this work.

Figure 2. Experimental Set-up of IGA-001 used for the measurements of Gas absorption/desorption.

Figure 3. Isothermal absorption and desorption of CO₂ in [MOA][Tf₂N]: (◇) absorption, (□) desorption at 303.15 K; (Δ) absorption, (x) desorption at 313.15 K; (●) absorption, (○) desorption at 323.15 K; and (+) absorption, (- -) desorption at 333.15 K. The points joined by the (.....) lines are points obtained by model estimates using parameters regressed from measured data.

Figure 4. Isothermal absorption and desorption of CO₂ in [BMIM][Tf₂N]: (◇) absorption, (□) desorption at 303.15 K; (Δ) absorption, (x) desorption at 313.15 K; (●) absorption, (○) desorption at 323.15 K; and (+) absorption, (- -) desorption at 333.15 K. The points joined by the (.....) lines are points obtained by model estimates using parameters regressed from measured data.

Figure 5. Isothermal absorption and desorption of CO₂ in [BMIM][MeSO₄]: (◇) absorption, (□) desorption at 303.15 K; (Δ) absorption, (x) desorption at 313.15 K; (●) absorption, (○) desorption at 323.15 K; and (+) absorption, (- -) desorption at 333.15 K. The points joined by the (.....) lines are points obtained by model estimates using parameters regressed from measured data.

Figure 6. Isothermal absorption and desorption of O₂ in [MOA][Tf₂N]: (◇) absorption, (□) desorption at 303.15 K; (Δ) absorption, (x) desorption at 313.15 K; (●) absorption, (○) desorption at 323.15 K; and (+) absorption, (- -) desorption at 333.15 K. The points joined by the (.....) lines are points obtained by model estimates using parameters regressed from measured data.

Figure 7. Isothermal absorption and desorption of O₂ in [BMIM][Tf₂N]: (◇) absorption, (□) desorption at 303.15 K; (Δ) absorption, (x) desorption at 313.15 K; (●) absorption, (○) desorption at 323.15 K; and (+) absorption, (- -) desorption at 333.15 K. (■) Anthony et al. (2005)²². The points joined by the (.....) lines are points obtained by model estimates using parameters regressed from measured data.

Figure 8. Isothermal absorption and desorption of O₂ in [BMIM][MeSO₄]: (◇) absorption, (□) desorption at 303.15 K; (Δ) absorption, (x) desorption at 313.15 K; (●) absorption, (○) desorption at 323.15 K; and (+) absorption, (- -) desorption at 333.15 K. The points joined by the (.....) lines are points obtained by model estimates using parameters regressed from measured data.

Figure 9. Figure: Isothermal absorption of CO₂ in [MOA][Tf₂N] in comparison to other ionic liquids measured in literature: (●) absorption at 313.15 K; (▲) absorption, at 323.15 K; (■) absorption at 333.15 K; (x) Absorption in [HMPY][Tf₂N] at 298.15 K³⁴; (o) [Grey] Absorption in [BMIM][PF₆] at 323.15 K⁴⁹; (o) Absorption in [HMIM][Tf₂N] at 323.15 K (Anderson et al.⁵⁰); (□) Absorption in [BMPY][Tf₂N] at 333.15 K⁴⁷

Figure 10. Isothermal absorption of CO₂ in [BMIM][Tf₂N] in comparison to other ionic liquids measured in literature: (■) Absorption at 303.15 K; (▲) Absorption at 313.15 K; (●) Absorption at 323.15 K; (◆) Absorption at 333.15 K; (x) Absorption in [HMPY][Tf₂N] at 298.15 K (Muldoon et al. 2007); (o) [Grey] Absorption in [BMIM][PF₆] at 323.15 K (Shiflett

et al. 2005); (o) Absorption in [HMIM][Tf₂N] at 323.15 K (Anderson et al. 2007); (◇) Absorption in [BMPY][Tf₂N] at 333.15 K (Kumelan et al. 2010)

Figure 11. Isothermal absorption of O₂ in [BMIM][Tf₂N] and [MOA][Tf₂N] in comparison to [BMPY][Tf₂N] measured in literature: (◆) Absorption in [BMIM][Tf₂N] at 303.15 K (▲) Absorption in [BMIM][Tf₂N] at 313.15 K; (■) Absorption in [MOA][Tf₂N] at 303.15 K (●) Absorption in [MOA][Tf₂N] at 313.15 K; (x) Absorption in [BMPY][Tf₂N] at 298.15 K (Anderson et al., 2007)

Figure 1.

(a)

(b)

(c)

Figure 2.

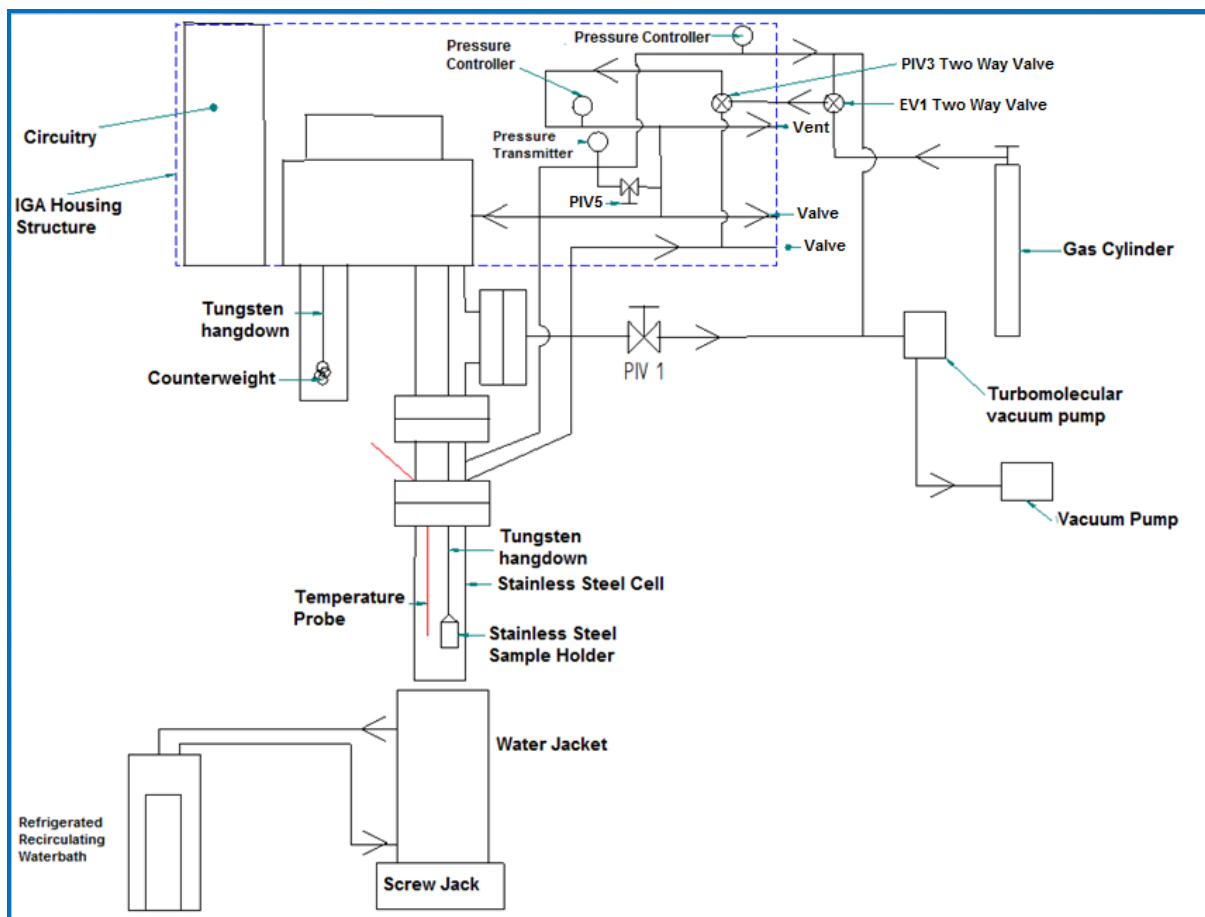


Figure 3.

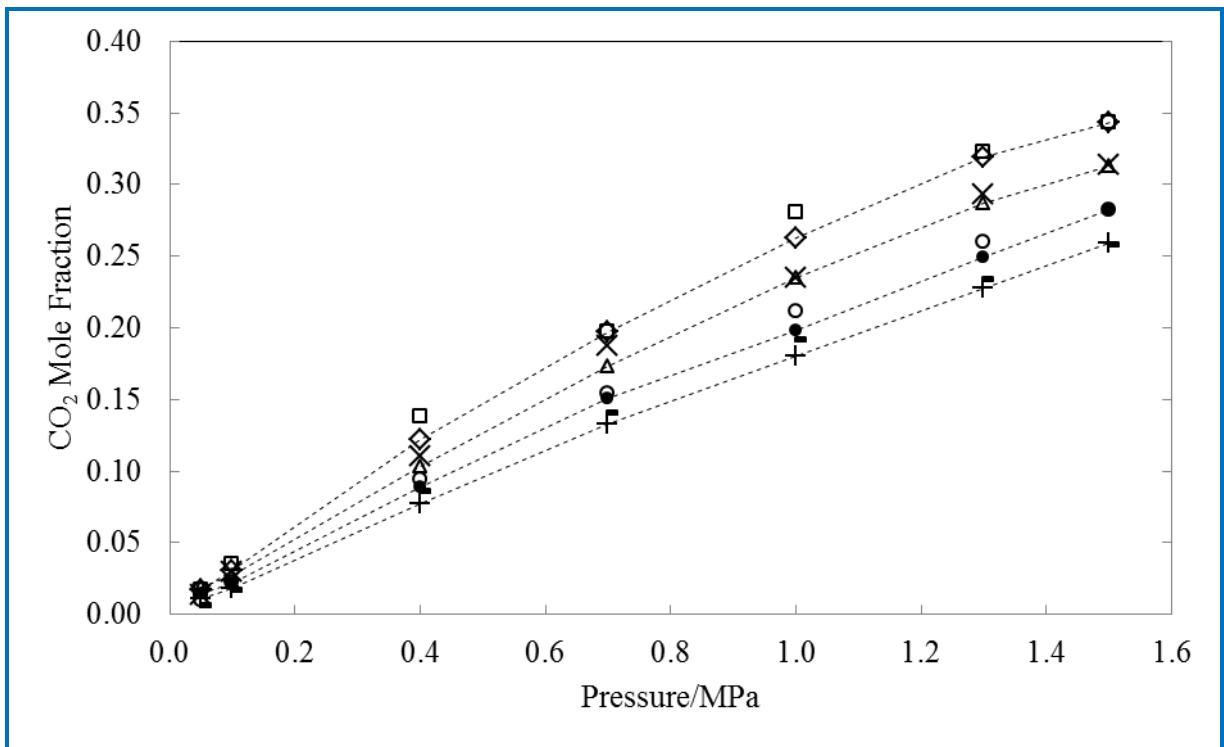


Figure 4.

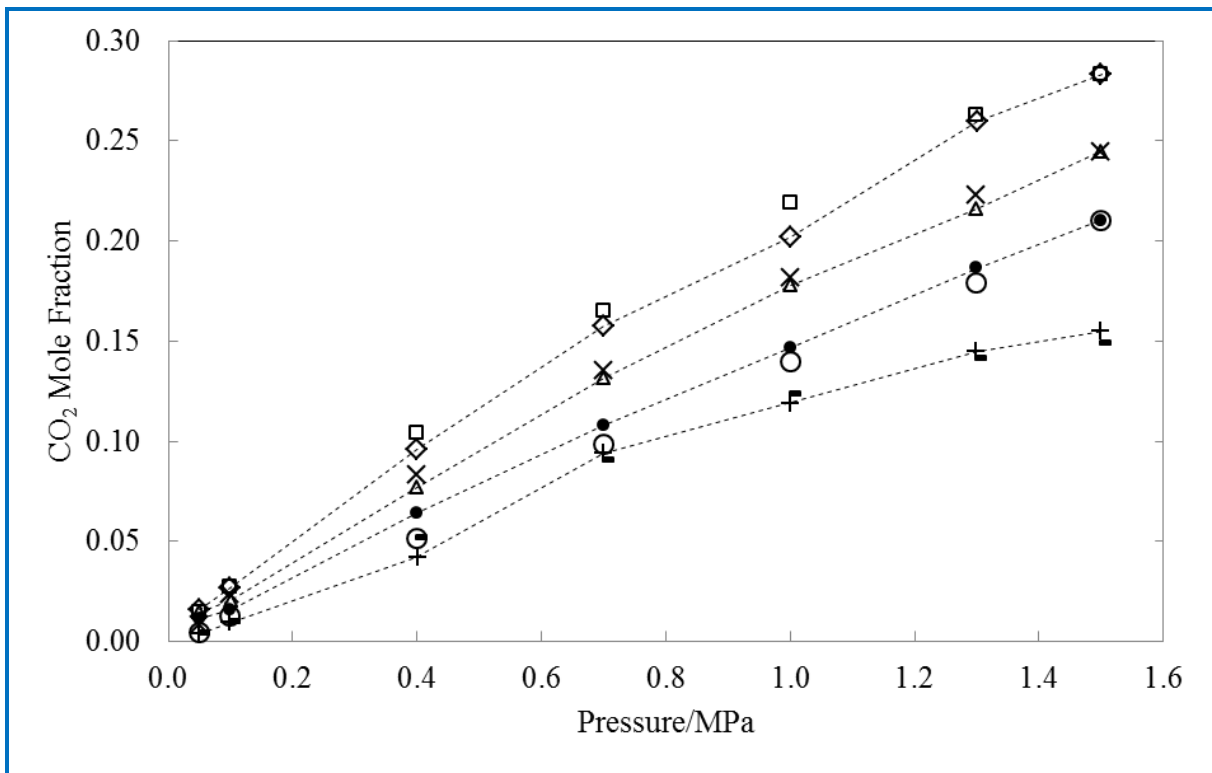


Figure 5.

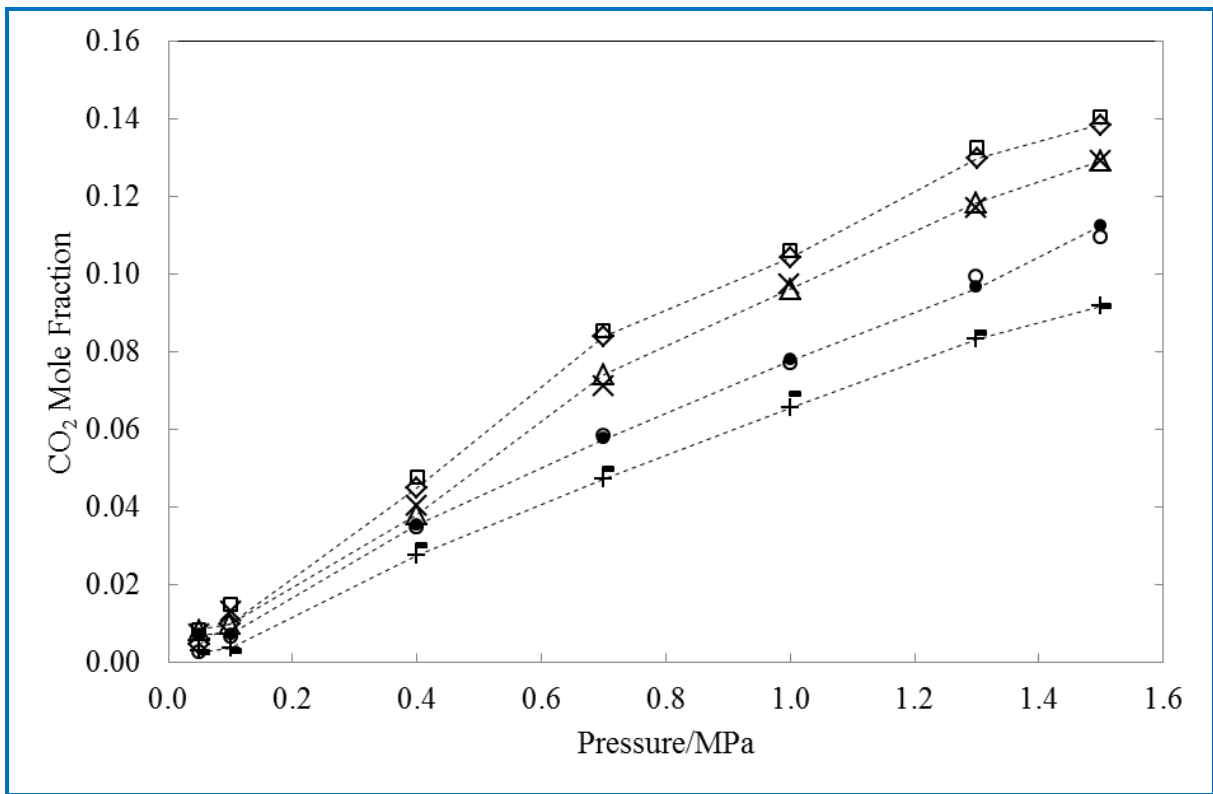


Figure 6.

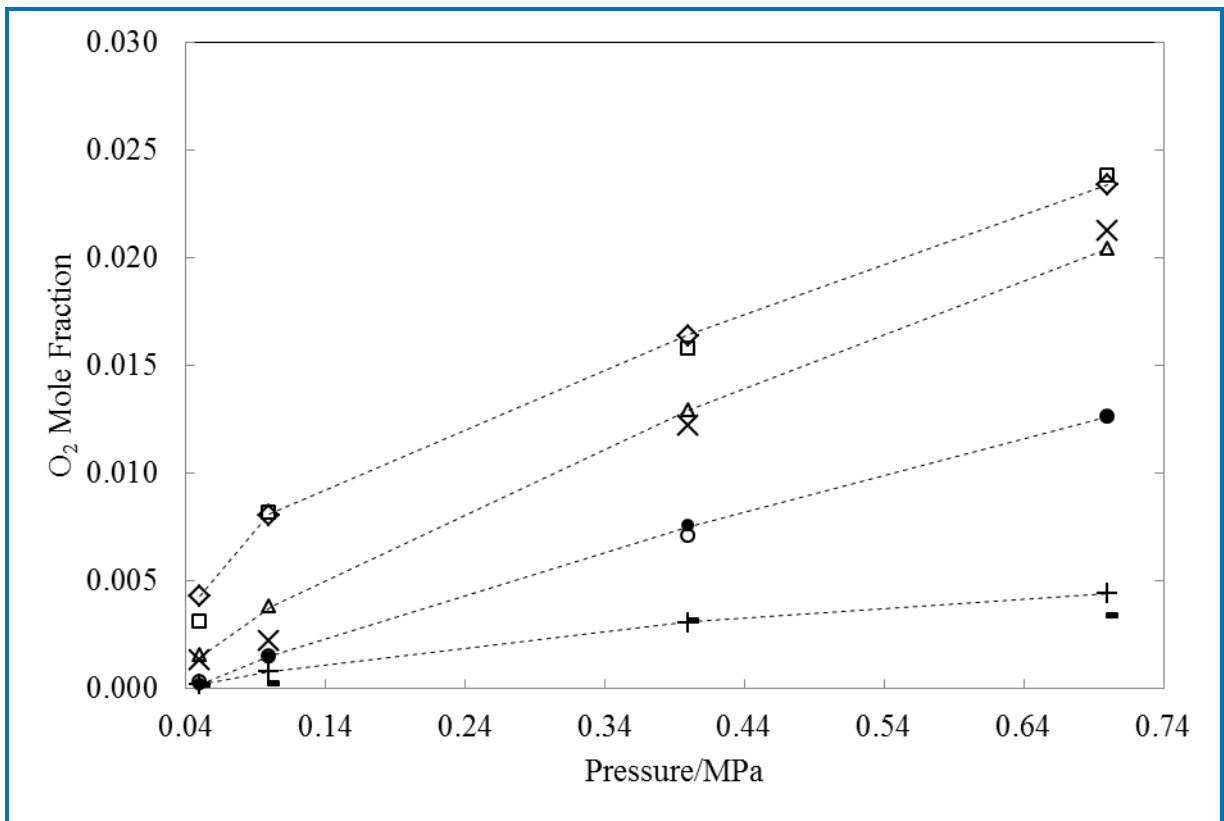


Figure 7.

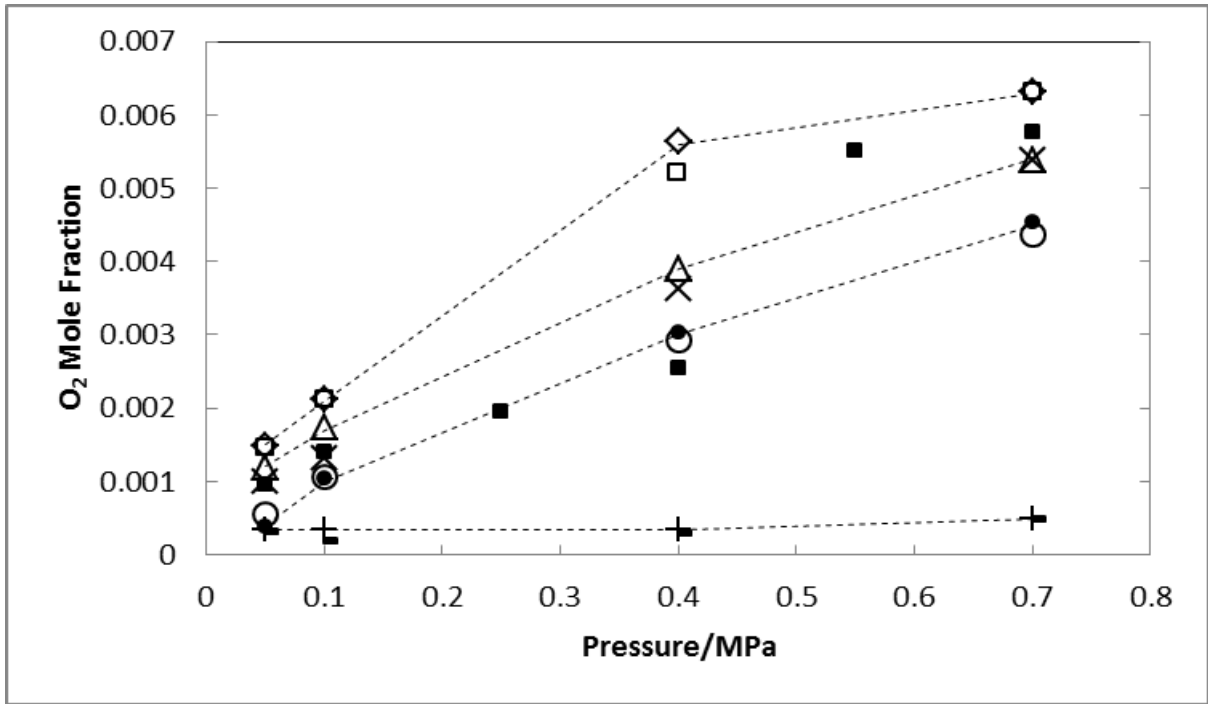


Figure 8.

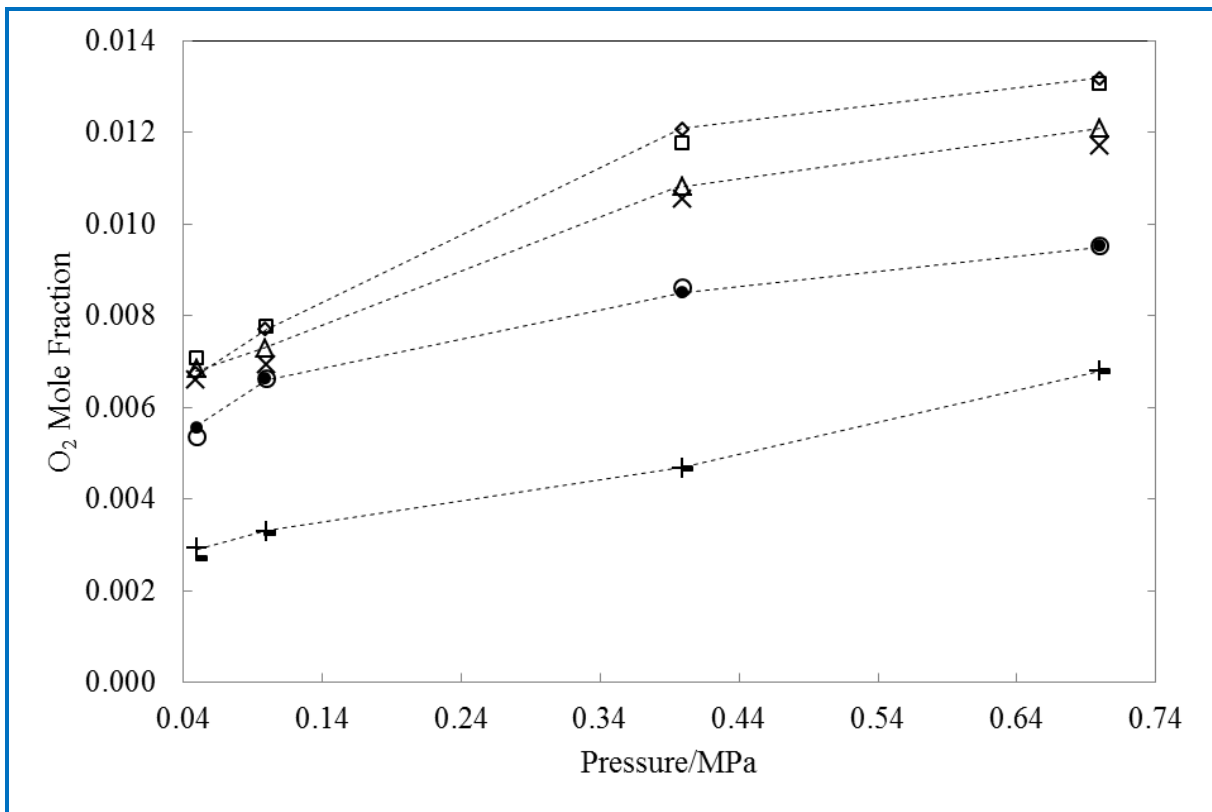


Figure 9.

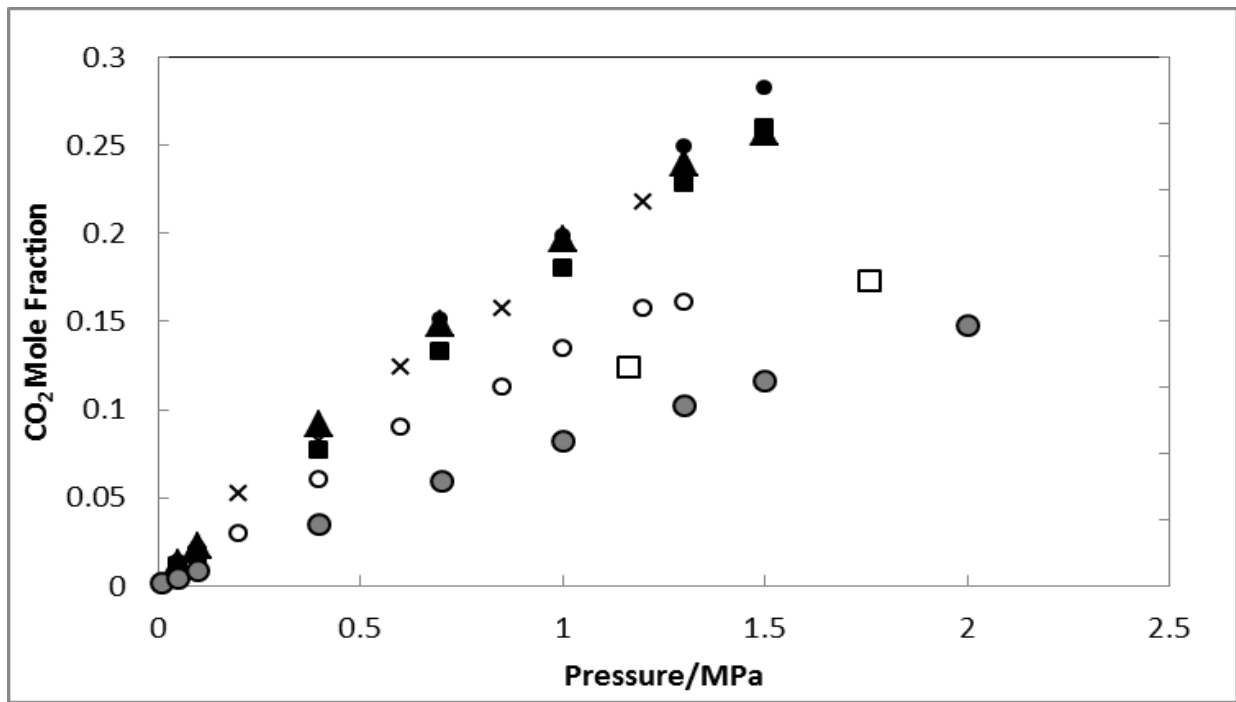


Figure 10.

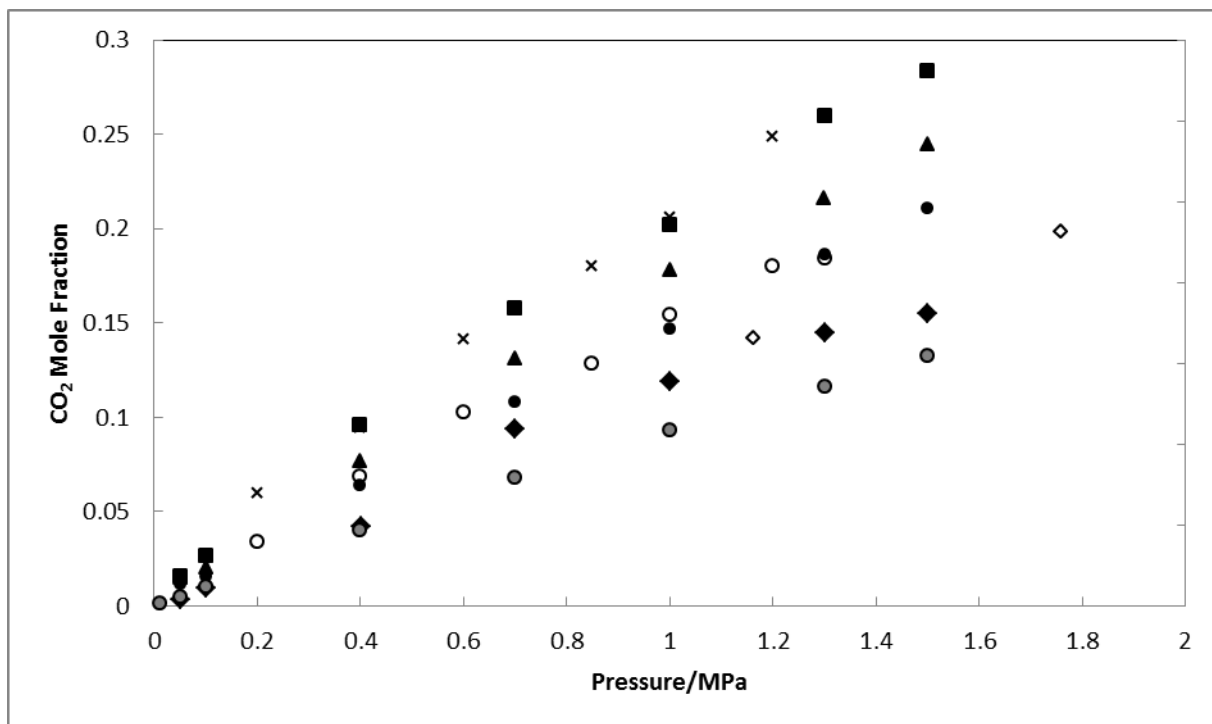
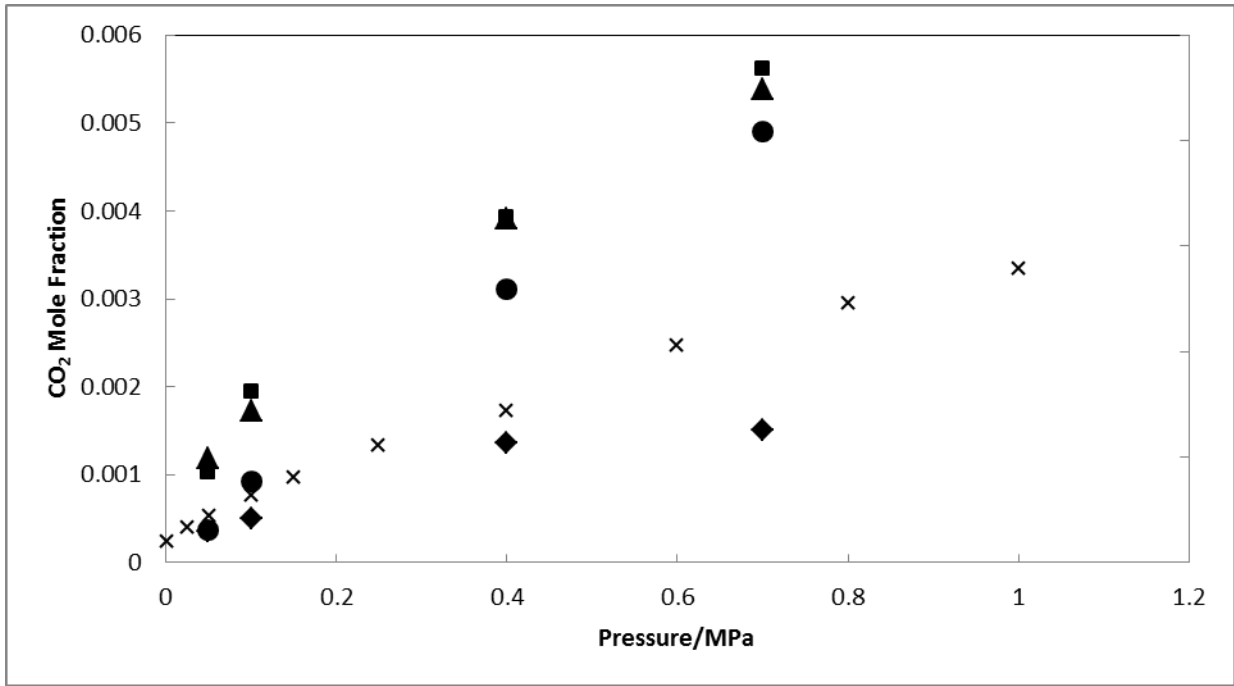


Figure 11.



Supporting information: Buoyancy Correction

The weight change of the sample as gas absorption/desorption occurs is calculated by taking into account all contributing forces including the mass of the counterweight and its associated attachments (hook and chain), the sample container and its associated attachments (hook and chains), the density of the sample and that of the absorbing gas. The following equation applies:

$$W = g[m_s + m_a - m_c + m_I - m_{II} - \rho_f(V_{as} + V_I - V_{II} - V_C)] \quad (1)$$

where W is the weight reading, g is acceleration due to gravity in $m.s^{-2}$, m_s is the dry sample mass, m_a is the mass absorbed which needs to be determined, m_c is the mass of counterweight, m_I and m_{II} are the mass of the balance components on the sample side and counterweight side respectively, and ρ_f is the density of the absorbing gas. All masses and the weight reading W are measured in grams. V_I , V_{II} and V_C are the volume of balance

components on the sample side, the volume of balance components on the counterweight side, and the volume of the counterweight respectively. V_{as} is the volume of the sample and the absorbed gas. All volumes are measured in cm^3 .

$$W = g[m_s + m_{a,N_2} - m_c + m_I - m_{II} - \rho_{N_2}(V_{N_2} + V_I - V_{II} - V_c)] \quad (2)$$

where m_{a,N_2} is the mass of sample and absorbed nitrogen and V_{N_2} is the volume of sample and absorbed nitrogen.

The method of buoyancy correction is explained in detail by Macedonia et al.,⁴⁸ In this study, the buoyancy of the sample was corrected using N_2 gas, which is negligibly soluble in the samples in question and possesses a molecular mass more comparable to CO_2 than the use of helium gas, thus providing good accuracy is asserting the assumption of $V_{as}=V_{N_2}$.

The error in weight measurement can be expressed as:

$$u(w) = u(w)^1 + u(w)^2 \quad (3)$$

where $u(w)^1$ and $u(w)^2$ is the sum of error in mass reading of each component in eqs 1 and 2, respectively.

Due to each mass of each balance component in eq 1 being accurate to ± 0.001 mg, and with the need of buoyancy correction eq 2, $u(w)$ may be expressed as:

$$u(w) = u(w)^1 + u(w)^2 = 0.005 + 0.005 = \pm 0.01 \text{ mg} \quad (4)$$

Table S1: Binary Interactions and Fitting Parameters by using RK-EOS model

T/ (K)	β_0	β_1	β_2	β_3	ℓ_{12}	ℓ_{21}	τ_{12}	m_{12}	σ
--------	-----------	-----------	-----------	-----------	-------------	-------------	-------------	----------	----------

CO ₂ (1) + [MOA][Tf ₂ N] (2)									
303.15	1.5x10 ⁻¹	-2.3x10 ⁻²	0.0	0.0	1.5x10 ⁻¹	1.0x10 ¹⁴	-2.3x10 ⁻²	9.1x10 ⁻¹	7.1x10 ⁻⁶
313.15	1.5x10 ⁻¹	-2.3x10 ⁻²	0.0	0.0	1.5x10 ⁻¹	1.0x10 ¹⁴	-2.3x10 ⁻²	9.1x10 ⁻¹	7.1x10 ⁻⁶
323.15	1.5x10 ⁻¹	-2.3x10 ⁻²	0.0	0.0	1.5x10 ⁻¹	1.0x10 ¹⁴	-2.3x10 ⁻²	9.1x10 ⁻¹	7.1x10 ⁻⁶
333.15	1.5x10 ⁻¹	-2.3x10 ⁻²	0.0	0.0	1.5x10 ⁻¹	1.0x10 ¹⁴	-2.3x10 ⁻²	9.1x10 ⁻¹	7.1x10 ⁻⁶
CO ₂ (1) + [BMIM][Tf ₂ N] (2)									
303.15	6.4x10 ⁻²	8.4x10 ⁻⁴	0.0	0.0	-2.2x10 ⁻¹	1.2x10 ¹	-8.8x10 ²	0.3x10 ¹	1.4x10 ⁻⁴
313.15	6.4x10 ⁻²	8.4x10 ⁻⁴	0.0	0.0	-2.2x10 ⁻¹	1.2x10 ¹	-8.8x10 ²	0.3x10 ¹	1.4x10 ⁻⁴
323.15	6.4x10 ⁻²	8.4x10 ⁻⁴	0.0	0.0	-2.2x10 ⁻¹	1.2x10 ¹	-8.8x10 ²	0.3x10 ¹	1.4x10 ⁻⁴
333.15	6.4x10 ⁻²	8.4x10 ⁻⁴	0.0	0.0	-2.2x10 ⁻¹	1.2x10 ¹	-8.8x10 ²	0.3x10 ¹	1.4x10 ⁻⁴
CO ₂ (1) + [BMIM][MeSO ₄] (2)									
303.15	1.7x10 ⁻¹	-1.7x10 ⁻²	0.0	0.0	9.9x10 ⁻¹	9.9x10 ⁻¹	7.25x10 ⁵	7.18x10 ³	1.5x10 ⁻⁴
313.15	1.7x10 ⁻¹	-1.7x10 ⁻²	0.0	0.0	9.9x10 ⁻¹	9.9x10 ⁻¹	7.25x10 ⁵	7.18x10 ³	1.5x10 ⁻⁴
323.15	1.7x10 ⁻¹	-1.7x10 ⁻²	0.0	0.0	9.9x10 ⁻¹	9.9x10 ⁻¹	7.25x10 ⁵	7.18x10 ³	1.5x10 ⁻⁴
333.15	1.7x10 ⁻¹	-1.7x10 ⁻²	0.0	0.0	9.9x10 ⁻¹	9.9x10 ⁻¹	7.25x10 ⁵	7.18x10 ³	1.5x10 ⁻⁴
O ₂ (1) + [MOA][Tf ₂ N] (2)									
303.15	-1.7x10 ⁻¹	4.3x10 ⁻²	0.0	0.0	-6.4	-8.7x10 ¹	-1.1x10 ⁻⁵	2.1	0.0
313.15	1.2	-2.3x10 ⁻¹	0.0	0.0	7.2x10 ⁻⁸	-3.5x10 ⁻⁶	6.8x10 ¹	9.7x10 ⁻¹	6.3x10 ⁻⁴
323.15	3.3	-4.9x10 ⁻¹	0.7	-0.2	0.0	0.0	-3.7x10 ⁵	5.6x10 ¹	2.5x10 ⁻⁵
333.15	1.7	1.4x10 ⁻¹	1.2	-0.3	-8.0x10 ⁻³	1.8	-3.0x10 ²	9.9x10 ⁻¹	1.5x10 ⁻⁴
O ₂ (1) + [BMIM][Tf ₂ N] (2)									
303.15	5.5	-1.4	0.0	0.0	6.3x10 ⁻¹⁰	-9.9x10 ⁻⁸	-5.4x10 ²	1.2	5.0x10 ⁻⁵
313.15	1.2	-3.0x10 ⁻¹	0.0	0.0	-6.2x10 ⁻³	1.2	-1.0x10 ²	9.9x10 ⁻¹	5.0x10 ⁻⁵
323.15	1.2x10 ²	-4.9x10 ¹	1.0	1.0	-4.2x10 ⁻⁷	-6.1	-2.5x10 ⁴	3.9x10 ¹	5.0x10 ⁻⁵
333.15	1.1x10 ²	-4.8x10 ¹	1.0	1.0	7.8x10 ⁻⁴	2.8x10 ³	8.6x10 ⁶	8.0x10 ²	2.5x10 ⁻⁵
O ₂ (1) + [BMIM][MeSO ₄] (2)									
303.15	9.9	-3.1	0.0	0.0	-1.2	-3.5	-1.1	1.0x10 ⁻¹	1.7x10 ⁻⁴
313.15	3.4	-1.1	0.0	0.0	-5.0x10 ⁻²	4.1	-2.0x10 ⁻¹	1.0	2.0x10 ⁻³
323.15	1.0	-1.2x10 ¹	1.0	1.0	-5.2 x10 ⁻²	-3.1x10 ⁵	-3.2x10 ²	1.0	1.5x10 ⁻⁴
333.15	2.9	-1.3 x10 ¹	1.0	1.0	-3.9x10 ⁻⁹	5.7x10 ⁻⁷	-6.5x10 ¹	-2.5	1.8x10 ⁻⁴

Table S2: Critical Properties of ILs used in this study

ionic liquid	molar mass/(g.mol ⁻¹)	T_b /K	T_C /K	P_C /bar	V_C /(cm ³ .mol ⁻¹)	ω
[MOA][Tf ₂ N]	648.85	1190.0	1447.35	10.31	2002.30	1.0096
[BMIM][Tf ₂ N]	419.37	784.6	1133.41	25.69	956.02	0.3526
[BMIM][MeSO ₄]	250.32	595.0	877.42	35.51	663.94	0.3913

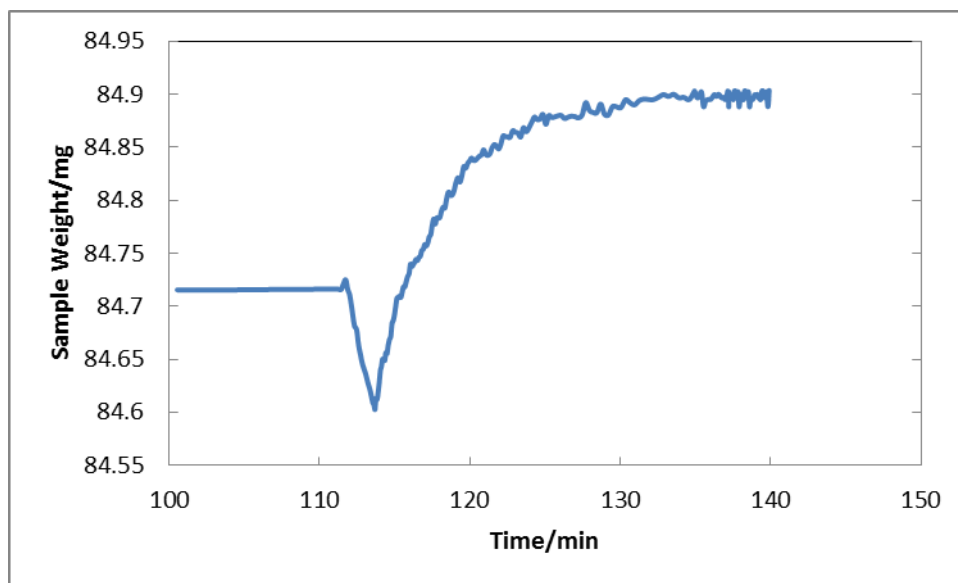


Figure S-1: Kinetic data of sample weight for CO₂ solubility in [MOA][Tf₂N] at 303.15 K and at 0.05 MPa